THE JOURNAL OF PHYSICAL CHEMISTRY B

Article

pubs.acs.org/JPCB

Complex Formation in Aqueous Trimethylamine-*N*-oxide (TMAO) Solutions

Johannes Hunger,[†,‡] Klaas-Jan Tielrooij,[†,∥] Richard Buchner,[§] Mischa Bonn,[†,‡] and Huib J. Bakker*[,†]

[†]FOM Institute AMOLF, Science Park 104, 1098 XG Amsterdam, The Netherlands

[‡]Max Planck Institute for Polymer Research, Ackermannweg 10, 55128 Mainz, Germany

[§]Institut für Physikalische und Theoretische Chemie, Universität Regensburg, 93040 Regensburg, Germany

ABSTRACT: We study aqueous solutions of the amphiphilic osmolyte trimethylamine-*N*-oxide (TMAO) using broadband dielectric spectroscopy and femtosecond mid-infrared spectroscopy. Both experiments provide strong evidence for distinctively slower rotation dynamics for water molecules interacting with the hydrophobic part of the TMAO molecules. Further, water is found to interact more strongly at the hydrophilic site of the TMAO molecules: we find evidence for the formation of stable, TMAO·2H_2O and/or TMAO·3H_2O complexes. While this coordination structure seems obvious, the lifetime of these complexes is found to be extraordinarily long (>50 ps). The existence of these long-lived complexes leads to pronounced parallel dipole correlations between water and TMAO, reflected in enhanced amplitudes in the dielectric spectra. The strong interaction between water and TMAO also results in a red-shifted band for the O−D stretching vibration of HDO molecules in an isotopically diluted aqueous TMAO solution. This O−D stretching vibration has a vibrational lifetime of 670 fs, which is significantly shorter than the lifetime of the O−D stretch vibration of bulk-like HDO molecules, presumably due to efficient coupling to vibrational modes of TMAO. The rotational dynamics of these O−D groups are slowed down dramatically, and are limited by the rotation of the whole complex, while the O−D vector oriented away from TMAO probably shows an accelerated reorientation.

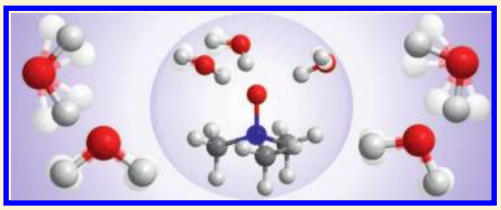

I. INTRODUCTION

Osmolytes are small molecules that play an important role in regulating the volume of living cells. They can counteract external osmotic or hydrostatic pressure and thereby prevent cells from shrinking.[1] Besides ions, proteins, or sugars, trimethylamine-*N*-oxide (TMAO) is a prominent organic molecule with osmolytic activity. TMAO is a common product of metabolism in living organisms and is in particular present in sea organisms. It is found in living cells up to very high concentrations without significant effects on the cell metabolism.[2] This is only possible because TMAO has a strong protein stabilizing effect,[3] which is essential for the biological function of proteins to remain intact.[4] Remarkably, the mechanism by which TMAO and other solutes affect protein stability, either positively or negatively, is still under debate. On the one hand, it has been suggested that denaturants directly interact with proteins, thereby affecting their structure and stability.[5,6] On the other hand, it has been proposed that osmolytes operate in a more indirect way, modifying the structure of the surrounding water, which in turn affects the stability of dissolved proteins.[7,8]

These two different scenarios have stimulated many theoretical[9−17] and experimental studies,[8,18−29] which have specifically focused on aqueous solutions of TMAO. In these studies, it was shown by various techniques that TMAO has a distinct effect on dynamics of water molecules that make up its hydration shell. In particular, time-resolved infrared experiments,[24,27] dielectric spectroscopy,[18] NMR-relaxation studies,[25] and molecular dynamics (MD) simulations[12] indicate that the rotational dynamics of part of the water molecules in an aqueous solution of TMAO are slowed down compared to bulk water. However, there is still a disagreement between experiments and simulations on the magnitude and the molecular origin of the retardation.[12,14,17,25] On the one hand, MD simulations find that hydrophobic groups only slightly slow down water dynamics,[12] while from polarization and time-resolved infrared experiments a more pronounced slowing-down of the rotational dynamics of water around the hydrophobic region was concluded.[24,27] The latter experiments were supported by 2D-IR experiments that show significantly slower spectral dynamics of the O−H stretch band for HDO molecules in solutions of amphiphilic molecules.[29]

In contrast to other amphiphilic molecules, like tetramethylurea (TMU),[30] the stabilization of proteins is rather unique to TMAO.[31] Compared to other amphiphiles, the hydrophilic fragment of TMAO is highly polar with significant partial charges located at the oxygen atom. In one of the resonant molecular structures of TMAO, three lone-pairs are located at the oxygen atom. Thus, the hydrophilic N−O group can accept up to three hydrogen-bonds. This suggests that the exceptional hydrophilic fragment of TMAO plays an important role in the protein stabilization mechanism. Accordingly, we report a study of the dynamics of aqueous TMAO solutions focusing on the

Received: December 28, 2011
Revised: March 11, 2012
Published: March 29, 2012

   dx.doi.org/10.1021/jp212542q | *J. Phys. Chem. B* 2012, 116, 4783−4795

interaction of water with the hydrophilic N−O group using two independent techniques. We report on dielectric relaxation spectroscopy (DRS) experiments that are sensitive to all solution dynamics that bring about a change of the macroscopic dipole moment.[32−35] By measuring the dielectric response at frequencies ranging from MHz to THz, we detect liquid dynamics over time scales spanning several orders of magnitude. We combine these results with polarization-resolved femtosecond infrared spectroscopy (fs-IR) experiments, which is a powerful tool to monitor the vibrational and reorientational dynamics of water molecules by labeling single molecules via vibrational excitation.[36−40]

II. EXPERIMENTAL SECTION

A. Dielectric Measurements. Dielectric spectroscopy probes the total polarization of a sample in a time-dependent electric field. The response of the sample is usually expressed as a function of the frequency, ν, in terms of the complex permittivity, $\hat{\varepsilon}(\nu) = \varepsilon'(\nu) - i\varepsilon''(\nu)$. Here, the relative permittivity, $\varepsilon'(\nu)$, represents the in-phase polarization of the sample and the dielectric loss, $\varepsilon''(\nu)$, is the out-of-phase response corresponding to the energy dissipation within the sample.

For the static case ($\nu = 0$), the molecular dipoles in a sample align along the externally applied field against the thermal motion, giving a polarization according to the static permittivity ε_s ($= \varepsilon'(\nu = 0)$) of the sample. As the frequency increases, an increasing number of molecular dipoles cannot follow the external field and $\varepsilon'(\nu)$ decreases to its high frequency limit ε_∞. Simultaneously, a characteristic peak in the dielectric loss, $\varepsilon''(\nu)$, is observed due to coupling of the molecular dipoles to the external field. For many dipolar liquids, this dispersion is observed at frequencies ranging from MHz to GHz and can be described with a Debye equation:[41]

$$\hat{\varepsilon}(\nu) = \frac{S}{1 + i2\pi\nu\tau} + \varepsilon_\infty \quad (1)$$

where τ is the relaxation time and S is the relaxation strength (amplitude). For a multicomponent system, multiple dispersions in $\varepsilon'(\nu)$ and peaks in $\varepsilon''(\nu)$ can be observed,[42] and each component is characteristic for the reorientation dynamics of the underlying dipolar species.

In the present study, complex permittivity spectra were measured in the frequency range $0.1 \lesssim \nu/\mathrm{GHz} \lesssim 1600$ at 25 °C. To cover this broad frequency range, several experimental techniques were combined.

At $0.4 \lesssim \nu/\mathrm{THz} \leq 1.6$, spectra were measured using a terahertz time-domain spectrometer (THz-TDS).[43] The spectrometer is based on terahertz generation in a ZnTe(110) nonlinear crystal, using the 800 nm pulses from a Ti-sapphire laser. The THz pulses transmitted through a quartz glass cuvette are recorded as a function of time, and a frequency domain analysis yields the complex index of refraction ($\hat{n} = n - ik$). From the indices of refraction, complex permittivity spectra, $\hat{\varepsilon}(\nu)$ ($= (\hat{n})^2$), were extracted. Measurements were recorded at 25 ± 1 °C. For details of the experiment, the reader is referred to ref 44.

Frequencies at $60 \leq \nu/\mathrm{GHz} \leq 89$ were covered with a variable path-length double-beam waveguide interferometer operating at 25.00 ± 0.05 °C. The interferometer is described in detail elsewhere.[45]

At $0.2 \lesssim \nu/\mathrm{GHz} \leq 50$, spectra were measured with a frequency-domain reflectometer based on an Agilent 85070E dielectric probe connected to an Agilent E8364B vector network analyzer (VNA).[46,47] Instrument drifts, due to thermal expansion of the cables, etc., were corrected for by an electronic calibration module (Agilent N4693B). Air, mercury, and water were used as primary calibration standards for the instrument. Calibration errors were corrected with a Padé approximation using propylene carbonate and *N*,*N*-dimethylacetamide as secondary standards.[48] The temperature was controlled to 25 ± 0.05 °C.

At high concentrations of TMAO, the spectra were extended with data at $0.1 \lesssim \nu/\mathrm{GHz} \leq 0.4$ using a time-domain reflectometer based on a Tektronix sampling scope (TEK 11802). The scope is connected to sampling heads (SD24) generating a fast rising (~17.5 ps) square wave signal at 200 kHz. The signal reflected from a cutoff type coaxial cell containing the sample is recorded as a function of time. Fourier transformation of the time traces yields the complex permittivity.[49] The cell and the feeding lines are immersed in a thermostat bath (25.00 ± 0.05 °C).

B. Femtosecond Infrared Measurements. Polarization-resolved femtosecond infrared spectroscopy is a powerful technique that can be used to selectively measure the reorientation dynamics of water molecules. This is achieved by using an intense mid-infrared pulse to excite the O−D vibration of an isotopically diluted sample (~8% HDO in H_2O). Excitation occurs most efficiently for those O−D groups whose transition dipole is aligned with the polarization of the exciting laser field, and thus, a subset of preferentially aligned O−D groups is tagged with a vibrational excitation. The evolution of the excitation and its angular distribution is monitored as a function of time, t, with a second variably delayed infrared probe pulse. For the probe pulse, the component parallel and perpendicular to the pump polarization can be selected, giving the parallel ($\Delta\alpha_\parallel(\omega,t)$) and perpendicular ($\Delta\alpha_\perp(\omega,t)$) transient (pump-induced) absorption spectra, respectively. From the measured absorption changes $\Delta\alpha_\parallel(\omega,t)$ and $\Delta\alpha_\perp(\omega,t)$, the isotropic signal can be constructed:

$$\Delta\alpha_{iso}(\omega, t) = \frac{\Delta\alpha_\parallel(\omega, t) + 2\Delta\alpha_\perp(\omega, t)}{3} \quad (2)$$

The isotropic signal is independent of reorientation processes and is dominated by the vibrational relaxation of the excitation and by the dynamics of any consecutive processes. For isotopically diluted water (8% HDO in H_2O), the excitation of O−D oscillators has been found to decay with a characteristic time constant of ~1.8 ps at ambient temperature.[50] The transient spectra associated with the excitation are dominated by a bleach ($\Delta\alpha_{iso} < 0$) at ~2510 cm^{-1} due to the depletion of the vibrational ground state population. In addition, the transient spectra show a superimposed induced absorption ($\Delta\alpha_{iso} > 0$) at $\omega < 2450$ cm^{-1} due to the excited-state absorption (i.e., the $1 \rightarrow 2$ transition that is spectrally shifted due to the anharmonicity in the O−D bond potential). After decay of the excitation, the vibrational energy dissipates in the solution to an intermediate state and eventually leads to heating of the sample by a few degrees. This heating effect dominates the transient spectra at long delays. Its associated spectrum corresponds to a thermal difference spectrum consisting of a bleaching signal at low wavenumbers and a blue-shifted induced absorption.[36,40,50]

Complementary to the isotropic signal, the anisotropy parameter $R(\omega, t)$ can be constructed:

$$R(\omega, t) = \frac{\Delta\alpha_{\parallel}(\omega, t) - \Delta\alpha_{\perp}(\omega, t)}{3\Delta\alpha_{iso}(\omega, t)} \quad (3)$$

$R(\omega, t)$ is solely sensitive to reorientation processes in the sample. The anisotropy parameter of the excitation (i.e., the measured anisotropy parameter corrected for the heating effect)[50] directly corresponds to the second-order rotational correlation time of HDO molecules, given that the vibrational lifetime and the transition dipole are independent of the molecular environment.[51] For neat water at ambient temperature, this characteristic reorientation time is 2.5 ps.[52]

Different subensembles of HDO molecules can be distinguished in the case of different isotropic spectral signatures or dynamics[53] and/or on the basis of distinctively different rotational dynamics.[54] fs-IR spectroscopy measures the second-order rotational correlation time, in contrast to dielectric relaxation spectroscopy, which measures first-order rotation times. As a result, the time constants measured with the two techniques differ by a factor of ~3.[52,55] This ratio is not exactly 3, because dielectric relaxation probes the macroscopic polarization, whereas the fs-infrared experiment probes the local dynamics. This effect increases the ratio of the first- and second-order rotational correlation time constants. In addition, for water, the reorientation takes place via large angle jumps.[56] This effect makes the ratio somewhat smaller. The net result of the two effects is that the ratio between the Debye time and the time constant measured in fs-infrared spectroscopy is ~3.4 for water.[52]

For the present study, pump and probe pulses were generated via a sequence of nonlinear optical conversion processes described in detail elsewhere.[57] These processes yield mid-infrared pulses with a duration of 150 fs and an energy of ~4 μJ at a repetition rate of 1 kHz. The pulses are split by a CaF_2 wedged window. The reflections at the front and the back sides of the wedged window are used as probe and reference pulses, respectively. The transmitted pulse (~90%) is used as the pump. With a $\lambda/2$ plate, the polarization of the pump pulse is set to an orientation of 45° with respect to the probe and the reference polarization. The time delay of the probe pulses with respect to the pump is varied via a variable path-length delay line. The three pulses are focused into the sample, which is held between two CaF_2 windows. The foci of the probe and pump overlap. After passing a polarizer used to select the parallel or perpendicular (with respect to the pump) polarization components, the probe and reference beams are sent into a spectrometer dispersing the beams onto a liquid-nitrogen-cooled mercury−cadmium telluride detector. The probe pulse is used to measure $\Delta\alpha_{\parallel}(\omega,t)$ and $\Delta\alpha_{\perp}(\omega,t)$. The reference pulse is used for a spectrally resolved correction of the pulse to pulse energy fluctuations.[57]

C. Materials. For DRS measurements, aqueous solutions of TMAO were prepared by adding degassed Millipore Milli-Q water to trimethylamine-*N*-oxide dihydrate (Fluka, >99%). For the fs-IR experiments, isotopically diluted (8% HDO in H_2O) solutions were prepared by adding a small amount of D_2O (Sigma-Aldrich, 99.9%) to an aqueous solution of TMAO. All solutions were prepared gravimetrically using an analytical balance.

D. Auxiliary Measurements. We measured TMAO solutions at concentrations, c, ranging from 0.24 to 5.9 mol L^{-1} (0.25 to 10 mol kg^{-1}). To calculate c from the molal concentration, m (in mol kg^{-1}), mixture densities were measured to an accuracy of ±0.05 kg m^{-3} using a vibrating-tube densimeter (Paar DMA60/601HT). Linear infrared spectra, $\alpha(\omega)$, were measured using a double beam mid-infrared spectrometer (Perkin-Elmer 881). The samples were contained between two CaF_2 windows separated by a Teflon spacer.

III. RESULTS

A. Dielectric Spectroscopy. For neat water at room temperature, the intense relaxation mode (bulk water mode) due to the rotation of the dipolar water molecules is centered at 20 GHz, corresponding to a relaxation time of 8.3 ps (Figure 1).[58] At THz frequencies, an additional weak high-frequency

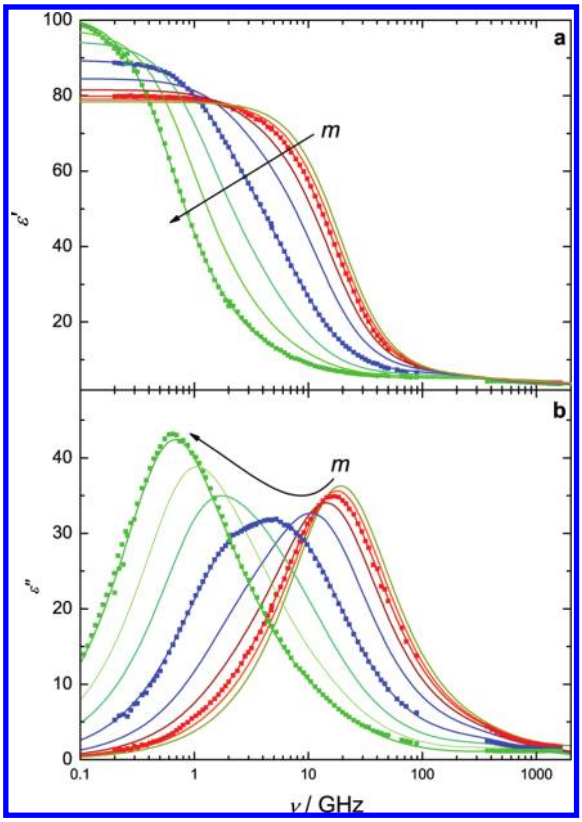

Figure 1. (a) Dielectric permittivity, $\varepsilon'(\nu)$, and (b) dielectric loss, $\varepsilon''(\nu)$, spectra for aqueous TMAO solutions at 25 °C. Symbols show experimental data (others omitted for visual clarity); lines represent the fit using eq 4; arrows indicate the increasing concentration of TMAO (0, 0.25, 0.5, 1, 2, 4, 6, 8, and 10 mol kg^{-1}).

mode (HF water mode) is observed that has been assigned to interaction-induced components in the water relaxation mechanism[59,60] or to a small angular rotation preceding a large angle jump.[61]

At low concentrations of TMAO, the peak in $\varepsilon''(\nu)$ is observed to be centered at ~20 GHz (Figure 1) as for neat water.[58] As the concentration of TMAO increases, we observe a shift of the maximum in $\varepsilon''(\nu)$ and of the dispersion in $\varepsilon'(\nu)$ to lower frequencies (Figure 1). This observation indicates a slowing down of the overall dynamics of the solution. Interestingly, a distinct double peak structure in $\varepsilon''(\nu)$ is observed at intermediate concentrations (e.g., at 4 mol kg^{-1}). This structure indicates the appearance of at least one slower

dx.doi.org/10.1021/jp212542q | J. Phys. Chem. B 2012, 116, 4783−4795

relaxation mode. The decrease in the dispersion and the dielectric loss observed at ~20 GHz show that the concentration of bulk-like water molecules decreases rapidly as m increases. Finally, close to the solubility limit of TMAO in water at ~10 mol kg^{-1}, the dielectric loss is dominated by an intense peak at ~700 MHz (corresponding to ~260 ps).

It is apparent from Figure 1 that the lower-frequency limit of $\varepsilon'(\nu)$ (i.e., the static dielectric constant, ε_s) increases from the value of neat water (ε_s = 78.4) to $\varepsilon_s \approx 100$ at 10 mol kg^{-1}. This finding is in agreement with an earlier, lower-frequency dielectric relaxation study on diluted aqueous TMAO solutions.[20] It is noteworthy that for an ideal (uncorrelated dipoles) mixture[42,62,63] of TMAO dipoles and water dipoles the static permittivity is expected to decrease. For this, we consider the effective dipole moment,[64] i.e., the dipole moment in the condensed phase including intramolecular polarization effects, of TMAO to be $\mu^{calc}_{eff,TMAO} \approx 6.8$ D (1 D = 3.33564 × 10^{-30} Cm), based on quantum mechanical *ab initio* calculations.[65] For the effective dipole moment of water, we assume $\mu^{exp}_{eff,H_2O} \approx 3.8$ D extracted from experimental dielectric spectra for water.[42,58] On the basis of these effective moments and the analytical concentrations of H_2O and TMAO in the mixture, a dielectric constant of $\varepsilon_s \approx 73$ would be expected for a mixture of 10 mol kg^{-1} TMAO in water. This contrasts the measured value of $\varepsilon_s \approx 100$, which leads us to conclude that pronounced (parallel) dipole−dipole correlations must occur in the binary mixtures. Thus, the polarization of the sample at low frequencies is significantly higher than it would be if it were solely due to independent alignment of TMAO and water dipoles to the external field. As we will show below, these correlations are due to the formation of TMAO·2H_2O and/or TMAO·3H_2O complexes, that results in a rigid alignment of water dipoles next to the hydrophilic group of TMAO.

1. Data Analysis. To explore the molecular origin of these observations, we model the experimental spectra. For aqueous solutions of TMAO, a separate relaxation related to the dipolar TMAO molecules is expected, in addition to the water response, which for neat water is formed by the modes at 20 GHz and ~0.5 THz. Further, it has been reported previously[12,14,17,24,25,27] that water molecules hydrating the TMAO molecule have distinctively slower rotational dynamics than bulk-like water molecules.

Taking these findings into account, we model the experimental dielectric spectra, $\hat{\varepsilon}(\nu)$, with a superposition of four Debye equations. It seems evident to interpret these two additional modes to the reorientational relaxation of, respectively, the TMAO molecules that are known to have a large dipole, and water molecules that have significantly slower dynamics compared to bulk water (slow water mode). Hence, the individual spectra were described by the following equation:

$$\hat{\varepsilon}(\nu) = \frac{S_{TMAO}}{1 + i2\pi\nu\tau_{TMAO}} + \frac{S_{slow}}{1 + i2\pi\nu\tau_{slow}} + \frac{S_{bulk}}{1 + i2\pi\nu\tau_{bulk}} + \frac{S_{HF}}{1 + i2\pi\nu\tau_{HF}} + \varepsilon_\infty \quad (4)$$

where S_j and τ_j are the relaxation strengths and relaxation times of each individual process, respectively. The infinite frequency limit, ε_∞, accounts for polarization effects (e.g., vibrations, librations, electronic polarization, etc.) above terahertz frequencies. Note that because of the nonlinear nature of the fitting procedure it is not possible to assign statistically meaningful standard uncertainties to the individual fit parameters.[66] Therefore, variations of the parameters between two independent measurements were taken as an indication for their reproducibility.

For the present spectra, indeed, four separate Debye-type relaxation modes give the lowest values of the reduced error function, χ^2,[64] whereas the assumption of only three relaxation modes yields somewhat higher values of χ^2.[67] Inclusion of an additional mode (i.e., five Debye-type relaxation modes) gives physically unreasonable parameters, e.g., negative amplitudes or relaxation times.

The contributions of each single relaxation mode to the dielectric loss spectra are depicted exemplarily at two different concentrations in Figure 2, and the obtained fitting parameters

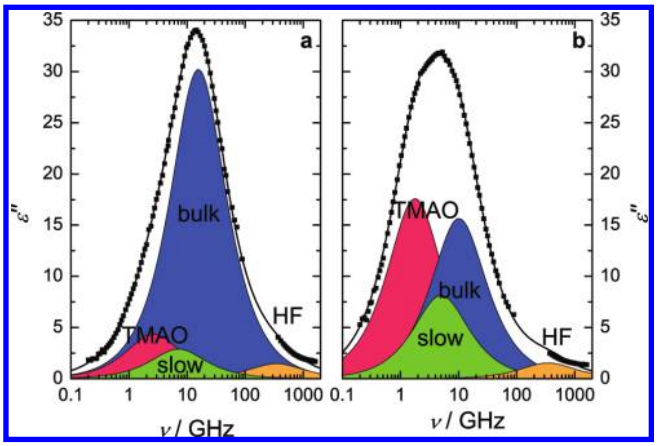

Figure 2. Dielectric loss spectra, $\varepsilon''(\nu)$, for a 1 mol kg^{-1} (a) and a 4 mol kg^{-1} (b) solution of TMAO in water at 25 °C. Symbols show experimental data, and solid lines correspond to the fit with eq 4. Shaded areas indicate the contributions of the four Debye modes (see text).

are shown as a function of concentration in Figure 3. We note that the concentration dependence for τ_{TMAO} parallels the variation for τ_{bulk} with c for low concentrations of TMAO. However, the slow water mode peaks between the intense TMAO relaxation and the strong bulk water mode, and is overlapped with these modes. Hence, its exact position in the data analysis is somewhat uncertain. In order to obtain more

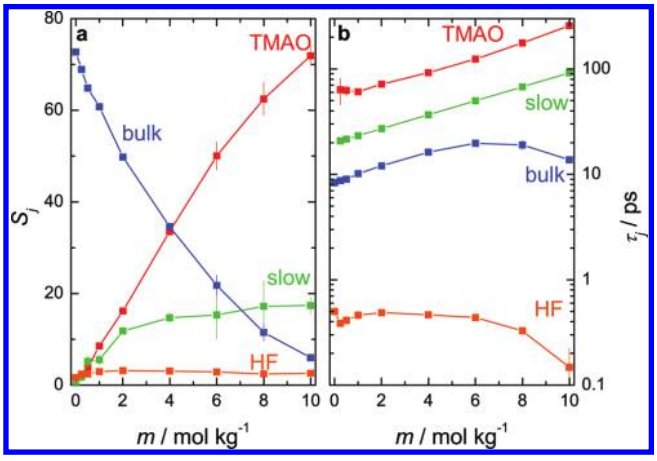

Figure 3. (a) Relaxation strength, S_j, and (b) relaxation times, τ_j, as a function of the molality, m, for the four Debye modes obtained by modeling the experimental permittivity spectra with eq 4. Error bars correspond to the variation within two independent measurements.

dx.doi.org/10.1021/jp212542q | J. Phys. Chem. B 2012, 116, 4783−4795

robust fit results, we limited the parameter space by assuming that τ_{slow} has the same concentration dependence as τ_{TMAO}; the latter can be unambiguously determined due to its high amplitude (S_{TMAO}). We hereby assume that the reorientation of molecular level dipoles is determined by the hydrodynamic environment and these hydrodynamic conditions are altered for all molecular species in a similar manner.

a. Water Relaxation. As for neat water,[58] a weak high-frequency mode centered at ~0.5 THz is observed at all concentrations. Its relaxation strength, S_{HF}, and the corresponding relaxation time, τ_{HF}, are essentially constant over the investigated concentration range (Figure 3). Since its molecular origin is likely related to an interaction-induced polarization of water[59,60] or to a small angular degree of freedom,[61] the data suggest that this mechanism is not significantly perturbed by the presence of TMAO.

At low concentrations of TMAO, we observe a pronounced relaxation at ~20 GHz as is observed in neat water (τ_{bulk} = 8.3 ps).[58] This mode is related to "bulk-like" water molecules. As already apparent from the raw spectra (Figure 1), we find a pronounced decrease in the relaxation amplitude, S_{bulk}, as the concentration of TMAO increases (Figure 3a). Its corresponding relaxation time, τ_{bulk}, increases smoothly up to 6 mol kg^{-1}. At higher concentrations, the data suggest that it decreases slightly, but due to the small amplitude at these concentrations, there is a relatively large uncertainty in the inferred relaxation times.

The amplitude of the bulk and fast relaxation modes described above only accounts for a fraction of the total number of water molecules in the solutions. Hence, we assign the remaining water fraction to water molecules located in the hydration shell of TMAO (slow water mode). We find the dynamics of these slow water molecules to be slower by a factor of 2−3 ($\tau_{slow} \approx 20$ ps) at low TMAO concentrations compared to bulk water ($\tau_{bulk} \approx 8.3$ ps). This finding is in agreement with the retardation due to hydrophobic groups as found for diluted solutions of tetramethylurea[54] or tetraalkylammonium salts.[68] For higher concentrations, the dynamics are further retarded and at 10 mol kg^{-1} the response attributed to slow water is centered at ~2 GHz ($\tau_{slow} \approx 90$ ps). Such a deceleration is commonly observed in the dielectric spectra for water molecules in the vicinity of hydrophobic moieties (hydrophobic hydration).[54,68,69] It is further in broad concordance with earlier studies on aqueous TMAO solutions using time-resolved infrared techniques,[24,27,29] while molecular dynamics simulations find a less pronounced deceleration at low solute concentrations.[10,12]

For quantitative analysis of the relaxation strengths, we use the Cavell equation[42] to relate S_j to the corresponding concentration of dipolar species:

$$\frac{2\varepsilon_s + 1}{\varepsilon_s} \cdot S_j = \frac{N_A c_j}{k_B T \varepsilon_0} \cdot (\mu_{eff,j}^{exp})^2 \quad (5)$$

This equation relates the amplitude S_j to molecular-level species[64] j of volume concentration c_j and effective dipole moment $\mu_{eff,j}^{exp}$ for a multicomponent dipolar mixture. The value $\mu_{eff,j}^{exp}$ corresponds to the dipole moment in solution and includes cavity- and reaction-field effects.[64] In eq 5, ε_s is the static permittivity ($= \varepsilon_\infty + \sum S_j = \lim_{\nu \to 0} \varepsilon'(\nu)$), N_A and k_B are the Avogadro and Boltzmann constants, T is the temperature, and ε_0 is the permittivity of free space.

By assuming the effective dipole moment of water, μ_{eff,H_2O}^{exp}, to be the same as that for neat water,[46] we obtain from S_{slow} and S_{bulk} the corresponding concentrations of slow, c_{slow}, and bulk-like, c_{bulk}, water, respectively. From these values, we determine the fraction of bulk water $f_{bulk} = c_{bulk}/c_{H_2O}$ and slow water $f_{slow} = c_{slow}/c_{H_2O}$, where c_{H_2O} is the analytical water concentration (55 mol L^{-1} for neat water). As will be shown below, we can thus follow the interconversion between the different types of water as the TMAO concentration is varied. It turns out that S_{slow} and S_{bulk} account for most of the water molecules in the sample.

As already mentioned before, the fraction of bulk-like water decreases rapidly as the TMAO concentration increases (Figure 4). The amplitude (Figure 3), and consequently the number of

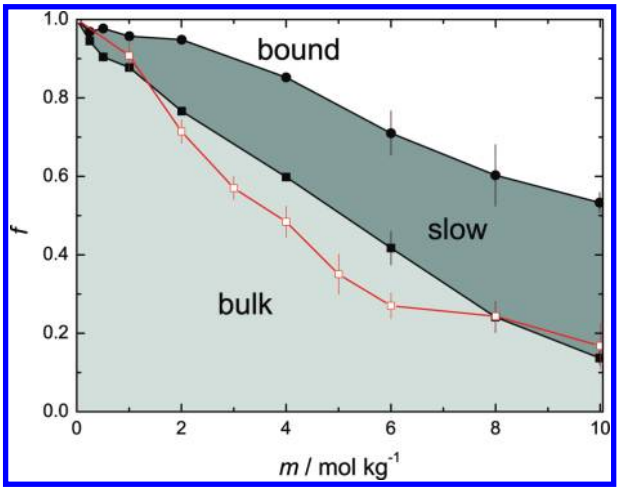

Figure 4. Fraction of bulk-like water, f_{bulk} (squares), and fraction of bulk-like water together with the slow water fraction, $f_{bulk} + f_{slow}$ (circles), as determined with dielectric spectroscopy (full black symbols). The bound fraction corresponds to water molecules that do not contribute to the water relaxation modes in the dielectric spectra (see text). Also indicated (open red symbols) is the fraction of bulk-like water as determined by fs-IR spectroscopy. The error bars correspond to the variation within two independent measurements.

water molecules in the proximity to a hydrophobic entity (Figure 4), increases smoothly and continuously as the concentration of TMAO molecules increases at low concentrations. Above ~4 mol kg^{-1}, a less steep increase is observed which suggests the onset of overlapping hydration shells. The observed fraction of slow water molecules corresponds to 5−9 H_2O per TMAO for dilute solutions. This value for water molecules in the vicinity of the hydrophobic moiety is in broad concordance with 8−12 H_2O for tetramethylurea,[54] taking the different numbers (3, respectively 4) of methyl groups of the two amphiphiles into account. It is also consistent with 9−10 water molecules as inferred from the MD simulations of ref 10 but somewhat lower than suggested by linear infrared spectroscopy (~17 H_2O)[21] and resulting from the MD simulation studies (~19−25 H_2O) of refs 12 and 25. At higher concentrations, the number of water molecules engaged in the slow water relaxation mode decreases, and at 10 mol kg^{-1}, only ~2 H_2O per TMAO can be detected in this mode. This is in line with overlapping hydrophobic hydration shells at high concentrations.

As can be seen from Figure 4, there is a significant difference between the water molecules that contribute to the water relaxation modes (bulk and slow water) and the analytical

dx.doi.org/10.1021/jp212542q | J. Phys. Chem. B 2012, 116, 4783−4795

concentration of water, c_{H_2O} (i.e., $f_{bulk} + f_{slow} < 1$). This means that there is a fraction f_{bound} (= $1 - f_{bulk} - f_{slow}$) of water molecules that has a significantly longer rotation time than that of the slow and bulk water molecules. To be more precise, the "missing" fractions of water molecules are very likely bound to TMAO, and do not contribute to the slow nor the bulk water relaxation modes (similar to water molecules in the hydration shell of cations[34]). The missing water portion can be converted to hydration numbers, Z_{ib} (= $(c_{H_2O} - c_{slow} - c_{bulk})/c$), that is, the number of bound water molecules per TMAO. We thus obtain $Z_{ib} \approx 2-3$ H_2O per TMAO molecule (Figure 5b). The

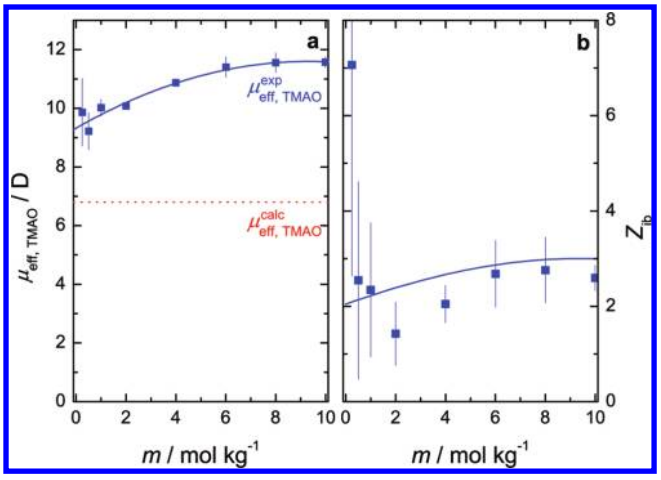

Figure 5. (a) Effective dipole moments, $\mu^{exp}_{eff,TMAO}$, of the lower frequency relaxation mode obtained using eq 5. The symbols correspond to experimental values, and the solid blue line represents a polynomial fit. The dashed red line represents the liquid phase dipole moment of TMAO $\mu^{calc}_{eff,TMAO}$ = 6.8 D as obtained with *ab initio* calculations.[65] (b) Irrotationally bound water molecules per TMAO molecule, Z_{ib} (see text). The solid line corresponds to the number of bound water molecules, as inferred from $\mu^{exp}_{eff,TMAO}$ using the dipole moments for TMAO·2H_2O and TMAO·3H_2O. The error bars correspond to the variation within two independent measurements.

observation of bound water molecules is in agreement with an earlier dielectric spectroscopy study by Shikata and Itatani[20] who observed ~2 bound water molecules per TMAO at $c < 1$ mol L^{-1}. As will be discussed below, these water molecules are bound in stable complexes with the solute TMAO. This finding is consistent with molecular dynamics simulations[10,12] and a linear infrared spectroscopic study[19] that shows that the hydrophilic entity of TMAO forms 2–3 strong hydrogen-bonds to water.

b. TMAO–Water Relaxation. The lowest-frequency mode is centered at $\nu \approx 2.7$ GHz ($\tau_{TMAO} \approx 60$ ps) for dilute solutions and is gradually shifting to lower frequencies as the concentration of TMAO increases. At the highest concentration of this study, m = 10 mol kg^{-1}, this mode peaks at ~0.7 GHz (τ_{TMAO} = 260 ps) and dominates the dielectric spectrum (Figure 1). As can be seen in Figure 3, the amplitude of the lowest-frequency mode, S_{TMAO}, increases monotonically with the concentration of TMAO. Due to the high amplitude and the location at low frequencies of this relaxation mode, we assign it to the dipolar TMAO molecule. This assignment is in line with earlier studies by Shikata and Itatani[20] and Freda et al.[18]

The value of $\tau_{TMAO} \approx 60$ ps for dilute solutions corresponds to a first-order microscopic rotational correlation time τ'_{TMAO} = 41 ps, using the Powles–Glarum equation[70,71] to correct for reaction field effects. Assuming a diffusive rotation mechanism, this is consistent with a second-order rotational correlation time of 14 ps for the N–O vector as found with MD simulations.[12] As the concentration of TMAO increases, τ_{TMAO} becomes longer (Figure 3). At 10 mol kg^{-1}, we find a value of τ_{TMAO} = 260 ps, corresponding to a microscopic first-order relaxation time of τ'_{TMAO} = 175 ps. This increase very likely represents the increasing viscosity of the solutions.[22,23]

To clarify the molecular-level origin of the relaxation mode, we use eq 5 to relate the observed relaxation strength, S_{TMAO}, to the dipole moment of the relaxing molecular-level species, $\mu^{exp}_{eff,TMAO}$. Assuming all TMAO molecules contribute to the relaxation mode ($c_j = c_{TMAO}$ in eq 5), we obtain an average value of $\mu^{exp}_{eff,TMAO}$ = 10.7 ± 0.3 D (Figure 5). This observed value is in broad accordance with an earlier study for diluted TMAO solutions that observed a value of 12 D.[20] However, the value is significantly higher than the dipole moment of a single TMAO molecule embedded in an effective medium with ε = 80, $\mu^{calc}_{eff,TMAO}$ = 6.8 D,[65] as obtained with *ab initio* quantum mechanical calculations. It is further inconsistent with the experimental value of the dipole moment for TMAO determined in apolar solvents (μ_{TMAO} = 5.04 D).[72] Together with the finding that there are 2–3 water molecules strongly bound (Figure 5b), the present results indicate that the underlying molecular-level species of the low-frequency relaxation mode are stable TMAO–water complexes, that have a larger dipole moment than an isolated TMAO molecule.

To test this hypothesis, we have performed quantum mechanical *ab initio* calculations[65] on a TMAO·3H_2O complex. The results of the geometry optimization for a TMAO·3H_2O complex in the gas phase and embedded in a continuum with ε_s = 80 (i.e., that of bulk water) are shown in Figure 6. In the gas

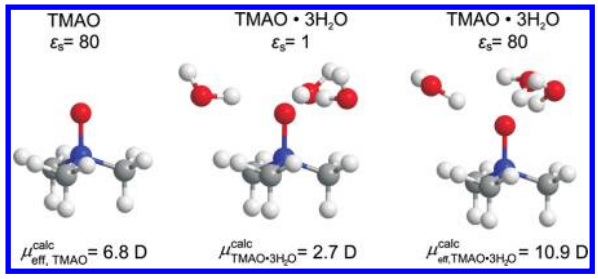

Figure 6. Structure and dipole moment of TMAO embedded in a medium with permittivity ε_s = 80, TMAO·3H_2O in the gas phase, and TMAO·3H_2O embedded in a continuum with permittivity ε_s = 80 as obtained with *ab inito* quantum mechanical calculations.[65]

phase, the minimum energy structure for a TMAO·3H_2O complex is obtained by a partial cancellation of the water and TMAO dipole vectors. This partial antiparallel alignment of the single molecule dipoles results in a decrease in $\mu^{calc}_{TMAO\cdot 3H_2O}$ for the complex, which is in agreement with previous calculations.[20,73] In contrast to the gas-phase results, calculations in a continuum of permittivity ε_s = 80[65] yield a partial parallel alignment of the molecular dipoles of water and TMAO (Figure 6). This parallel alignment of the molecular level dipoles (and a partial charge transfer from TMAO to water)[73,74] yields a value of $\mu^{calc}_{eff,TMAO\cdot 3H_2O}$ = 10.9 D for the dipole moment of the TMAO·3H_2O complex. This value is in remarkably good agreement with the experimentally observed effective dipole moments $\mu^{exp}_{eff,TMAO}$ = 10.7 ± 0.3 D. Since both

dx.doi.org/10.1021/jp212542q | J. Phys. Chem. B 2012, 116, 4783–4795

the experimental value and the calculation in the continuum include local-field effects, they are directly comparable. Hence, the findings collectively indicate that the hydrophilic part of TMAO can strongly bind 3 H_2O for concentrated aqueous solutions, with the TMAO and water dipoles partially aligned.[75]

It may be significant that the observed value of $\mu^{exp}_{eff,TMAO}$ increases slightly as the concentration of TMAO increases (Figure 5). This points either toward some dipole−dipole correlations between TMAO·3H_2O complexes or to a gradual change from TMAO·2H_2O at low concentrations to TMAO·3H_2O for concentrated solutions. The latter is consistent with the somewhat lower dipole moment obtained for a TMAO·2H_2O complex.[75] Using the calculated dipole moments for the TMAO·2H_2O and TMAO·3H_2O complexes, we estimate the number of bound water molecules from the observed value for $\mu^{exp}_{eff,TMAO}$. Within the experimental precision, these values are consistent with the number of bound water molecules, Z_{ib}, as determined from the fraction of bound water molecules (Figure 5b). It is important to note that a formation of TMAO·2H_2O complexes at low concentrations and TMAO·3H_2O at high concentrations does not directly imply a change in the coordination structure of the TMAO molecules but rather points toward a lengthening of the lifetimes for the water−TMAO hydrogen-bonds with concentration (see Discussion below). The formation of stable TMAO·3H_2O complexes also explains the observed increase in the static permittivity with concentration (Figure 1a).

B. Femtosecond Infrared Spectroscopy. *1. Linear Infrared Spectra.* For neat HDO in H_2O (8% HDO in H_2O), the linear infrared spectrum shows two distinct bands at frequencies ranging from 2100 to 2600 cm^{-1} (Figure 7). The

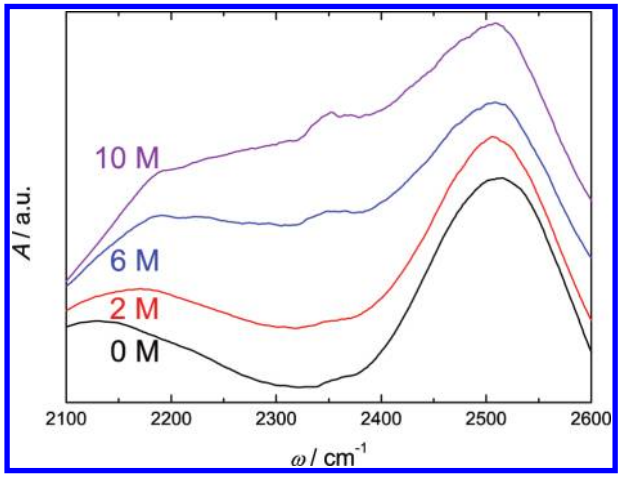

Figure 7. Linear infrared spectra at frequencies characteristic for the O−D stretching vibration for solutions of TMAO in isotopically diluted water (8% HDO in D_2O). The spectra are offset vertically for clarity.

O−D stretching vibration is centered at ~2510 cm^{-1}, and at ~2100 cm^{-1}, a weaker band due to a combination vibration of H_2O is observed.[76] For aqueous solutions of TMAO (8% HDO in H_2O), a pronounced asymmetric broadening toward lower wavenumbers for the O−D stretching vibration of HDO is observed (Figure 7). A similar broadening has previously been observed for the O−H stretching vibration.[19,77] These red-shifted stretching oscillators correspond to water molecules that are engaged in strong hydrogen-bonds. In agreement with the claimed formation of very strong hydrogen-bonds between water and TMAO,[8,10,14,77] and confirmed by the DR results indicating stable TMAO−water complexes, we assign the red-shifted O−D oscillators to HDO molecules that form strong hydrogen-bonds to the hydrophilic part of TMAO. For the O−H stretching vibration, a similar asymmetric broadening has been observed which has been described with an additional red-shifted band. Its center frequency is not very well-defined and has been reported at 2970 cm^{-1} (ref 19) and at 3200 cm^{-1} (ref 77). Its contribution to the infrared spectra has been found to correspond to ~2 water molecules per TMAO, consistent with the composition of the TMAO−water complexes inferred from our DR experiments.

2. Isotropic Transient Absorption. We investigate the dynamics of the HDO molecules that are strongly hydrogen-bonded to TMAO using femtosecond infrared spectroscopy. In contrast to our previous studies,[24,27] we use red-shifted pump and probe pulses centered at ~2450 cm^{-1}, where the contribution of the red-shifted band dominates, as evident from the linear infrared spectra.

Figure 8 shows that the transient spectra are dominated by a bleach of the fundamental transition but no induced absorption.

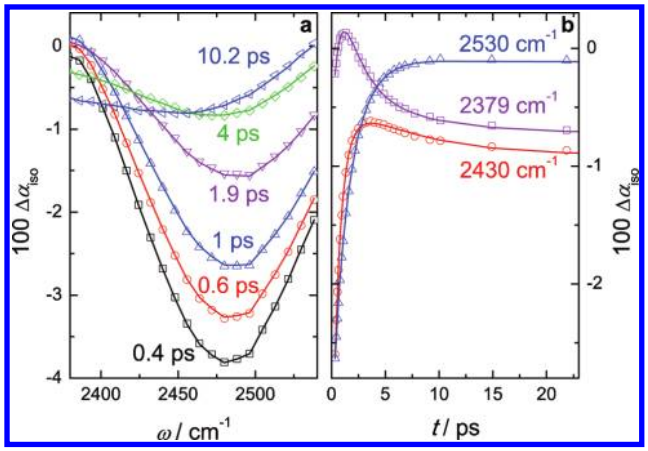

Figure 8. (a) Transient absorption spectra, $\Delta\alpha_{iso}(\omega)$, for a 10 M solution of TMAO in isotopically diluted water (8% HDO in H_2O) at different delays after excitation. (b) Delay scan, $\Delta\alpha_{iso}(t)$, for a 10 M solution of TMAO for three selected frequencies. The symbols correspond to experimental data, and the lines represent the fits with the kinetic model (see text).

This suggests that at $\omega \lesssim 2450$ cm^{-1} an additional bleaching signal is superposed onto the excited state absorption of bulk HDO molecules and is indicative of a red-shifted band (in addition to the O−D stretching band of bulk water) as already apparent from the linear spectra. Second, the maximum bleached signal in $\Delta\alpha_{iso}$ shifts to higher wavenumbers as t increases for early delays (<3 ps in Figure 8a). This observation points at the presence of two distinct bands, a red band with a short lifetime of the excitation and a second band at higher wavenumbers with a somewhat slower vibrational decay. This is supported by the delay traces depicted in Figure 8b that show a significantly faster decay at early delays (<5 ps) at 2430 cm^{-1} compared to 2530 cm^{-1}. The delay trace at 2379 cm^{-1} gives even stronger evidence for the presence of two distinct bands. At this frequency, we observe initially a bleaching signal, followed by an induced absorption ($\Delta\alpha_{iso} > 0$), and finally reaching a bleaching signal at long delays (Figure 8b). Such behavior cannot be reproduced with a single state decaying to a final end state (heat). In fact, this behavior shows that at early

dx.doi.org/10.1021/jp212542q | J. Phys. Chem. B 2012, 116, 4783−4795

delays the transient spectra are dominated by the bleach of a short-lived red-shifted band. As the excitation of this band decays, the measured signal is dominated by the excited-state absorption of the (longer-lived) blue-shifted band. Finally, as the excitation of both bands has decayed, the transient spectra are dominated by the heated end-state corresponding again to a bleaching signal.

Another interesting feature is observed at long delays, where the heating effect prevails. As indicated in Figure 8b, the transient spectra show still some variation with time at delays >20 ps and have not yet reached a final value. These slow dynamics become more pronounced as the concentration increases and are indicative of very slow heating dynamics for high concentrations of TMAO.

a. Data Analysis. For neat water, the rise of the thermal signal does not instantaneously follow the relaxation of the vibrational excitation but is somewhat delayed. This delay can be modeled by introducing an intermediate state that has no transient spectral signature at frequencies of the O−D stretching vibration (i.e., the absorption is the same as for the vibrational ground state).[36,78,79] To account for the red-shifted band, an additional excited state with a shorter lifetime is included. The further ingrowth of the heating effect is modeled using an additional state that has the same spectral signature as the heated end-state but a lower amplitude. A schematic representation of the kinetic model is depicted in Figure 9. The

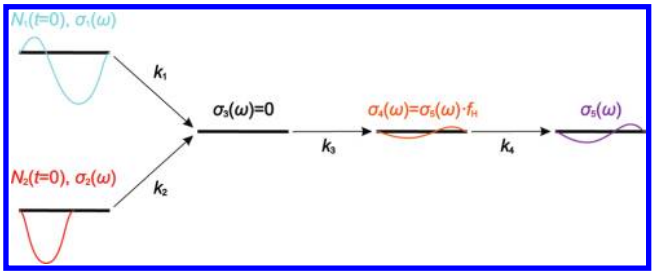

Figure 9. Schematic representation of the kinetic model used to describe the experimental transient isotropic spectra, $\Delta\alpha_{iso}(\omega,t)$, and a schematic representation of the relevant transient spectra (wiggly lines). The excitation of bulk water (with corresponding spectrum, $\sigma_1(\omega)$, and initial population, $N_1(t = 0)$) and of the red-shifted band ($\sigma_2(\omega)$, $N_2(t = 0)$) decay with characteristic rate constants k_1 and k_2, respectively, to a common intermediate state. The intermediate state has no transient spectral signature at frequencies of the present study ($\sigma_3(\omega) = 0$). The pump-pulse energy decays further to a heat state ($\sigma_4(\omega)$) that finally relaxes to the final end-state ($\sigma_5(\omega)$).

rate constants k_j and the spectra associated with each state are obtained by fitting the isotropic data $\Delta\alpha_{iso}(\omega,t)$ over the measured frequency and delay time range. In this fit, the rate constants, k_j, and thus the corresponding vibrational lifetimes, $\tau_{vib,j}$ (= $1/k_j$), are assumed to be constant over the investigated range of frequencies.

The initial populations of both exited states ($N_1(t = 0)$ and $N_2(t = 0)$) were chosen in order to obtain ~1.2 times higher cross sections for the red-shifted band compared to the bulk band at all concentrations. This ratio is based on the extensive study reported by Corcelli and Skinner.[80] Fits using this model are depicted for a 10 mol kg^{-1} solution of TMAO in isotopically diluted water in Figure 8.

b. Excited State Dynamics. In Figure 10a, we show the measured $\Delta\alpha_{iso}$ together with the decomposition into the two

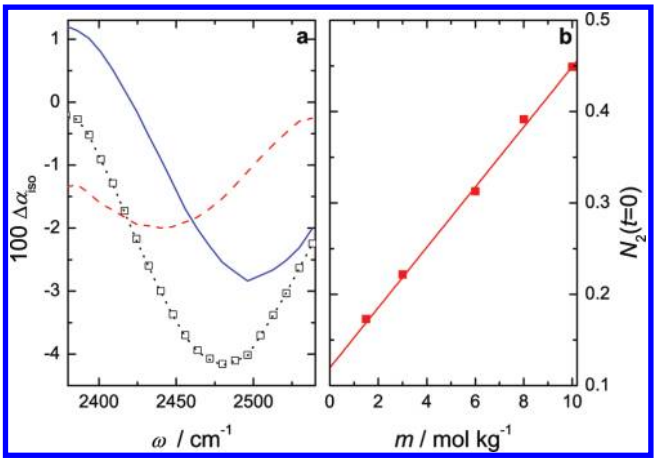

Figure 10. (a) Transient isotropic spectrum for a solution of 10 mol kg^{-1} TMAO measured 300 fs after excitation (symbols). The dotted black line represents the fit with the kinetic model (see text; Figure 9). Also shown are the contributions of the two excited states ($\sigma_1(\omega)$, solid blue line; $\sigma_2(\omega)$, dashed red line). (b) Relative population of the red-shifted band ($\sigma_2(\omega)$) to the measured transient spectra at t = 0, $N_2(t = 0)$. The symbols correspond to experimental values, and the line represents a linear fit.

bands σ_1 and σ_2 of the excited O−D vibrations at t = 300 fs, where the contribution due to the heating effect is negligible.

The spectral signature of the first excited state, σ_1, closely resembles the results for neat isotopically diluted H_2O with a characteristic bleach at $\omega \approx 2510$ cm^{-1} and an adjacent induced absorption due to excited state absorption at $\omega \approx 2400$ cm^{-1} (Figure 10a). The vibrational excitation decays with a characteristic rate of k_1 = (0.55 ± 0.03) ps^{-1} ($\tau_{vib,1}$ = (1.8 ± 0.1) ps). The value of k_1 is constant over the entire concentration range within the experimental accuracy. We reported previously[27] a moderate increase in the vibrational relaxation time scale. However, the present model showing no variation of the vibrational relaxation rates with concentration also perfectly describes our previous data, which did not focus on red-shifted wavenumbers.[27] The observed decay rate is in excellent agreement with the value measured for neat water (k_1 = 0.56 ps^{-1}).[50] Hence, these results suggest that the observed excited state corresponds to HDO molecules that are very similar to bulk-like water with respect to their hydrogen-bonded structure and vibrational coupling to the environment.

The spectrum of the second excited state, σ_2, corresponds to a bleaching signal with a Gaussian band-shape (Figure 10a). Its maximum bleach is centered at ω = (2450 ± 10) cm^{-1} at all concentrations. This band arises from HDO molecules that form strong hydrogen-bonds to the hydrophilic part of TMAO. The vibrational relaxation of this red-shifted band is approximately 3 times faster with a decay rate of k_2 = (1.5 ± 0.1) ps^{-1} ($\tau_{vib,2}$ = (670 ± 50) fs). At first sight, this may appear surprising, since the vibrational relaxation of O−D oscillators in neat H_2O has been found to be rather insensitive to the absorption frequency.[36,78] The fast decay of water molecules that are hydrogen-bonded to TMAO indicates that these water molecules have access to additional relaxation paths. These paths are very likely related to the TMAO molecules itself, e.g., involve coupling to TMAO combination modes.[81] The vibrational relaxation time $\tau_{vib,2}$ is found to be independent of TMAO concentration.

The initial populations at t = 0 are directly related to the concentration of the different subensembles of HDO molecules

dx.doi.org/10.1021/jp212542q | J. Phys. Chem. B 2012, 116, 4783−4795

in solution. Hence, the population $N_2(t = 0)$ corresponds to the fraction of O−D oscillators forming hydrogen-bonds to TMAO with respect to the overall number of O−D oscillators in solution (because $N_1(t = 0) + N_2(t = 0) = 1$). As can be seen in Figure 10b, this fraction increases linearly with TMAO concentration. At 10 mol kg^{-1} TMAO in water, a major fraction of the O−D groups that are excited with the red-shifted pump pulse are hydrogen-bonded to TMAO. Given the spectral overlap of the pump with the two bands, this is consistent with TMAO forming three hydrogen-bonds to H_2O.

c. Delayed Heating Dynamics. At late delays, we observe slow dynamics related to a further heat equilibration. These slow dynamics are only present for high concentrations of TMAO and are not observed at $m < 2$ mol kg^{-1}. As can be seen in Figure 11a, these slow dynamics correspond to an increase of

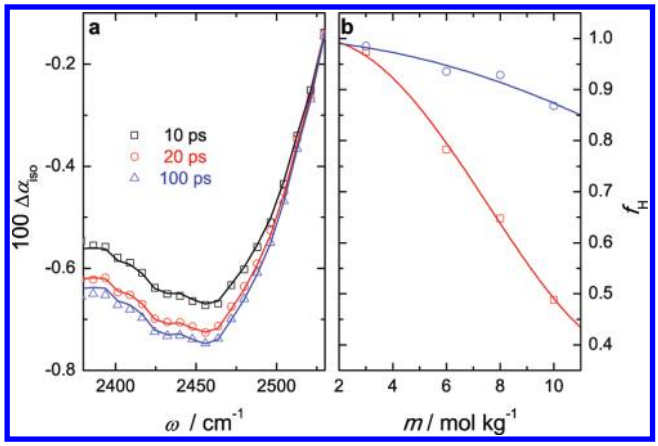

Figure 11. (a) Transient isotropic spectra for a solution of 8 mol kg^{-1} TMAO in isotopically diluted water at late delay times. The symbols show experimental data, and the lines correspond to the fit with the kinetic model (see text; Figure 9). (b) Scaling factor, f_H, for the intermediate heated state with respect to the heated end-level. The red squares and blue circles correspond to pump−probe experiments performed at 2440 and 2560 cm^{-1}, respectively. The lines are just a visual aid.

the magnitude of the heating signal. A second remarkable observation is that the magnitude of this delayed heating effect is significantly larger for pump−probe experiments performed at 2440 cm^{-1} than for experiments in which the pump pulse is centered at 2560 cm^{-1}.

The dependence on the pump frequency is consistent with an efficient coupling of HDO molecules in the vicinity of TMAO to vibrational modes of TMAO. These TMAO vibrations have apparently a relatively long lifetime, leading to a rather delayed appearance of some portion of the heating signal. For experiments performed at 2440 cm^{-1}, more HDO molecules close to the TMAO molecules are excited (compared to experiments with the pump frequency centered at 2560 cm^{-1}), which results in a large degree of excitation of the TMAO modes. As a consequence, the magnitude of the delayed heat ingrowth is higher. We observe the difference in magnitude between σ_4 and σ_5 to be strongly dependent on concentration (Figure 11b). The equilibration rate $k_4 = (0.09 \pm 0.05)$ ps^{-1} ($\tau_{vib,4} = (11 \pm 6)$ ps) is essentially constant at all concentrations and does not depend on the pump frequency. This indicates that the equilibration mechanism is solely dependent on the TMAO molecule and not on other solution properties.

3. Anisotropic Transient Absorption. a. Red-Shifted Band. As shown above, we find the absorption of O−D oscillators that form strong hydrogen-bonds to TMAO to be centered at $\omega \approx 2450$ cm (Figure 10a). From the isotropic results, we find that for high concentrations of TMAO the transient spectra are dominated by these molecules at early delay times. After decay of this excitation, the spectra are dominated by the excited state absorption of the bulk-like band centered at $\omega \approx 2510$ cm^{-1}. Hence, the anisotropy parameter at these frequencies is a superposition of the rotational dynamics of the red-shifted band and the center frequency absorption, weighted by their (time-dependent) contribution to the isotropic spectra.

In order to obtain the anisotropy parameter of the O−D groups, we subtract the heating contribution.[50] As can be seen in Figure 12a, for neat HDO in H_2O, $R(t)$ decays smoothly

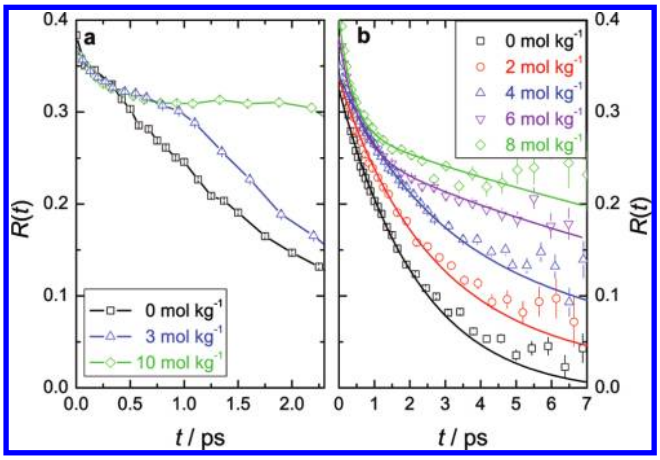

Figure 12. (a) Anisotropy parameter, $R(t)$, for the O−D vibration of HDO molecules in aqueous TMAO solutions as a function of delay time, t, for experiments with the pump pulse centered at $\omega \approx 2440$ cm^{-1}. (b) $R(t)$ for the O−D vibration of HDO molecules for experiments with the pump pulse centered at $\omega \approx 2560$ cm^{-1}. The symbols correspond to experimental data, and the lines correspond to fits according to eq 6.

with increasing delay time, when measuring the anisotropy on the red side of the band, at 2440 cm^{-1}. On the contrary, for a 10 mol kg^{-1} solution of TMAO, after a small initial decay, the anisotropy remains essentially constant for times up to 2.2 ps, for which the transient spectra are dominated by the excitation of the red-shifted band. This finding is in agreement with the rotational dynamics of these hydrogen-bonds being governed by the slow rotation of the entire TMAO·3H_2O complex. At intermediate concentrations (e.g., 3 mol kg^{-1}, Figure 12a), the red-shifted band dominates the transient spectra up to ~0.8 ps, while at later delay times the contribution of the red-shifted band is negligible. This is reflected in a step-like behavior of the observed anisotropy parameter (Figure 12a) where the slowly reorienting TMAO complexes prevail at short delay times. At longer delay times, $R(t)$ reflects the rotation of the other water molecules. We note that the measurements at these low frequencies are complicated by the excited state absorption of the 2510 cm^{-1} band; thus, we only consider the relative variation with TMAO concentration and we do not perform a quantitative analysis.

b. Center Frequency Absorption. In order to circumvent interference with the red-shifted band, we have tuned the pump frequency to higher wavenumbers ($\omega \approx 2560$ cm^{-1}; full width

dx.doi.org/10.1021/jp212542q | J. Phys. Chem. B 2012, 116, 4783−4795

at half-maximum ~110 cm^{-1}). As can be seen in Figure 12b, the anisotropies exhibit a continuous decay, indicating no significant contribution of the red-shifted band. There is a substantial speed-up at short times and slow-down at long times. We have previously attributed the speed-up at short delay times to accelerated rotation dynamics of the bulk water fraction.[27] Comparison with other solutes containing methyl groups has indicated that the slow-down at long times is due to water molecules close to the hydrophobic groups of the TMAO molecules.[24] The resulting $R(t)$ decays closely follow our earlier fs-IR studies;[27,50] therefore, we include these measured anisotropy decays in our analysis. We note that the O−D oscillators of HDO molecules that are engaged in a TMAO·3H_2O complex but oriented away from the TMAO molecules will presumably have a similar absorption spectrum and vibrational lifetime as a bulk-like HDO molecule. Hence, these HDO molecules will contribute to the anisotropy parameter of the center-frequency absorption. We assume these O−D groups to have similar rotation dynamics to bulk-like water molecules. As a consequence, we fit the measured $R(t)$ decays to a biexponential decay:

$$R(t) = A_{bulk} \cdot e^{(-t/\tau_{IR,bulk})} + A_{slow} \cdot e^{(-t/\tau_{IR,slow})} \quad (6)$$

In eq 6, A_{bulk} corresponds to the amplitude of bulk-like water molecules reorienting with a characteristic time, $\tau_{IR,bulk}$. A second portion, A_{slow}, of water molecules in the vicinity of a hydrophobic moiety shows much slower reorientation dynamics. We fix this slow rotational correlation time to the value obtained from the dielectric measurements after correction for the experimental difference in the rotational correlation times $\tau_{IR,slow} = \tau_{slow}/3.4$.[52] The thus resulting slow reorientation time $\tau_{IR,slow}$ amounts to 7 ps at 1 mol kg^{-1} and increases to 27 ps at 10 mol kg^{-1} TMAO in water. The corresponding fractions and the bulk-like reorientation time are the free parameters. At low concentrations of TMAO (m < 4 mol kg^{-1}), we fix $\tau_{IR,bulk}$ to the value measured for neat water ($\tau_{IR,bulk}$ = 2.5 ps).[50] As can be seen in Figure 12, our model excellently describes the experimental anisotropy decays. In agreement with our previous studies,[27] the bulk reorientation time, $\tau_{IR,bulk}$, decreases at concentrations above 4 mol kg^{-1}, and at 10 mol kg^{-1} of TMAO, we observe a value of $\tau_{IR,bulk}$ ~ 0.5 ps.

For a direct comparison with the results obtained with dielectric relaxation spectroscopy, we calculate the corresponding fractions of bulk-like water molecules, f_{bulk} (= (A_{bulk}/(A_{bulk} + A_{slow}))((110 − 3·m)/110)). This expression takes into account that the center frequency absorption band does not contain the O−D groups forming direct hydrogen-bonds to TMAO (~3). The factor 110 reflects the effective concentration of hydroxyl groups, i.e., twice the concentration of water molecules. In Figure 4, we show the fractions thus obtained together with the results obtained with dielectric spectroscopy. The fractions of bulk-like and slow water as inferred from the fs-IR anisotropies are in broad agreement with the DRS results. At intermediate concentrations, we detect a somewhat higher fraction of slow water, i.e., water hydrating the hydrophilic group, with fs-IR than with DR.

IV. DISCUSSION

The DRS results show that the molecular structure of aqueous TMAO solutions is dominated by pronounced dipole−dipole correlations, as indicated by the increase in the static permittivity, ε_s, with increasing concentration. In combination with quantum mechanical *ab initio* calculations, we show that these correlations originate in very strong hydrogen-bonds between a few water molecules and TMAO. The observed amplitude of the TMAO relaxation and the increase of the static permittivity with increasing concentration of TMAO evidence the existence of stable TMAO·2H_2O and/or TMAO·3H_2O complexes, with a strong correlation between the orientation of the dipoles of TMAO and water.

While the acceptance of three hydrogen-bonds by TMAO is rather intuitive and widely reported in the literature,[10,12,19,73,82] it is important to realize that, to be detectable as a separate relaxation mode in the dielectric spectrum, the lifetime of such a complex has to be longer than the observed rotational correlation times τ_{TMAO} = 60−260 ps (depending on concentration). If the lifetimes were shorter than the rotational correlation time of the complex, the dipolar TMAO and water molecules would contribute separately to the dielectric spectrum. This means that the dipole−dipole correlations leading to the increase of the dielectric strength would not be observed.

This immediately implies that the lifetime of a O−H···O−N hydrogen-bond is substantially longer than the lifetime of a water−water hydrogen-bond.[83] The fact that the lifetimes of these hydrogen-bonds are longer than the rotation time of the whole complex has already been postulated previously on the basis of nuclear Overhauser experiments.[22] MD simulations[8,14] predict a significantly longer hydrogen-bond lifetime for a water−TMAO than for a water−water hydrogen-bond, but the reported lifetimes are still far too short to be consistent with our findings. MD simulations predict the hydrogen-bonded lifetimes to be 4 (ref 14) to 7 (ref 8) times longer than a water−water hydrogen-bond. However, the nonpolarizable force field used in the MD simulations cannot accurately describe the interactions with water for the hydrophilic entity of TMAO, as reflected in the erroneous structures of TMAO hydrates.[84] These interactions include a significant charge transfer from TMAO to water[73,74] that cannot be captured by classical MD simulations. In this context, *ab initio* molecular dynamics simulations would be desirable, since these calculations can account for the partial charge transfer within the TMAO−H_2O bond.

The asymmetric broadening toward low wavenumbers of the linear infrared spectra is consistent with the presence of strong hydrogen-bonds between HDO molecules and TMAO (Figure 7). Our time-resolved infrared experiments allow us to spectrally resolve a separate infrared band, associated with these strong hydrogen-bonds, that is red-shifted by ~55 cm^{-1} with respect to neat HDO. We find that the strong hydrogen-bonds lead to a very efficient coupling between the excited HDO molecule and TMAO. This results in an effective decay mechanism of O−D groups directly interacting with the TMAO and as a consequence in an almost 3 times shorter vibrational lifetime of HDO molecules bound to TMAO ($\tau_{vib,2}$ = (670 ± 50) fs) compared to neat HDO in H_2O. In addition, the TMAO molecules appear to store the transferred vibrational energy very efficiently, leading to rather slow heating dynamics with a characteristic time of $\tau_{vib,4}$ = (11 ± 6) ps.

Both dielectric relaxation and polarization-resolved femtosecond infrared experiments reveal a pronounced slowing down of the rotational water dynamics, attributed to water located in the hydrophobic hydration shell of TMAO. For dilute solutions, the rotational dynamics of 5−9 water molecules

per TMAO are slowed down by a factor of 2−3 compared to neat water. As the concentration increases, the dynamics are further decelerated and at m = 10 mol kg^{-1} the rotational dynamics are approximately 10 times slower compared to neat water. These findings are in line with previous studies that have shown a slowing down of the water dynamics within the hydrophobic hydration shell of amphiphilic molecules, irrespective of the nature of the hydrophilic group.[24,27,29,54]

The DRS results indicate that the rotation dynamics of the water molecules bound to the hydrophilic moiety are largely determined by the rotation of the whole TMAO·2H_2O/TMAO·3H_2O complex. This is consistent with a rather time-independent anisotropy observed for O−D oscillators bound to TMAO as measured in the fs-IR experiments (Figure 12a), as rotation of these O−D groups require rotation of the whole complex, which is slow. Due to their short vibrational lifetime and the weakening of their bond strength, the slow rotational dynamics of these O−D oscillators contribute only at early delay times and at low wavenumbers (∼2450 cm^{-1}) to the observed anisotropies.

A striking difference between the DR and the fs-IR experiments is the acceleration of the rotational dynamics of "bulk-like" water molecules at high concentrations of TMAO in the fs-IR measurements.[27] This feature is very weak in the dielectric relaxation experiments (Figure 3b). To explain this difference, one has to keep in mind that fs-IR spectroscopy is sensitive to the rotational dynamics of the O−D transition dipole (i.e., the O−D vector), while DR spectroscopy monitors the rotation of the permanent dipole moment of water. These two vectors do not coincide.[34,44,85] Taking these distinctively different sensitivities of both experiments into account, the observations can be explained from the formation of stable TMAO·2H_2O/TMAO·3H_2O complexes. The acceleration of $\tau_{IR,bulk}$, as observed with polarization resolved fs-IR measurements, may originate in the rotation of some of the O−D oscillators within such a complex, presumably those oriented away from the hydrophilic N−O group. The likely origin for the speed-up is the disruption of the local hydrogen-bonded structure close to the hydrophilic parts of the TMAO−water complexes. For instance, the rotational dynamics of these O−D groups can be faster and not anymore determined by the rearrangement of the surrounding hydrogen-bond network due to local defects in the solution structure.

V. BIOLOGICAL IMPLICATIONS

As TMAO plays an important role in the regulation of the volume of a living cell by counteracting external osmotic pressure,[1,86] our results suggest that this biological function is closely related to the ability to strongly bind water molecules. Thus, by strongly binding three water molecules, TMAO reduces the activity of water inside a cell significantly and therefore reduces the activity gradient along the cell membrane. A similar mechanism has been found for TMAO counteracting the destabilizing effect of urea by directly binding urea molecules.[87,88]

As already mentioned in the Introduction, TMAO is an osmolyte, which is commonly used to stabilize proteins.[31] This means that TMAO can stabilize the tertiary structure by enhancing the intraprotein interactions, which are dominated by hydrophobic interactions and internal hydrogen-bonds.[89,90] In general, amphiphilic molecules can mediate the interaction between hydrophobic protein fragments and the surrounding aqueous environment via a direct mechanism.[7,39] The hydrophobic intraprotein interaction is thereby weakened, and the folded protein structure is destabilized. Our results suggest that for TMAO this direct destabilizing effect is of minor significance compared to the profound indirect stabilizing effect.[7,39] These stabilizing effects are related to the formation of the TMAO water complexes, which in turn lead to an enhancement of the polarity of the solution as reflected in the increase in the dielectric constant. Hence, the presence of TMAO makes the exposure of the hydrophobic protein fragments to the solvent less favorable and thereby promotes the interaction between hydrophobic entities of a protein. In addition, the strong interaction of the hydrophilic oxygen of TMAO may lead to an indirect stabilization of proteins. The formation of the long-lived water hydrogen-bonds to TMAO is highly exothermic,[73] and thus, interaction of water with TMAO is energetically favorable over hydration of a protein. This formation of strong hydrogen-bonds leads to a decrease of the activity of water in solution and causes dewetting of the biomolecule.[91] This means that TMAO can promote intra-protein interaction by lowering the number of available water molecules that are competing for hydration sites at the protein.[8,90,92]

It is noteworthy that the molecular structure of TMAO is quite similar to that of other amphiphilic molecules like, for instance, tetramethylurea (TMU) or *t*-butyl alcohol (TBA). Nevertheless, TMAO has a stabilizing effect on the folded protein conformation,[3] whereas TMU and TBA have a destabilizing effect.[30,93] The chemical difference between TMAO and other amphiphiles largely consists in the strength of the interaction between their hydrophilic group and water. For TMU and TBA, the interaction between the hydrophilic moiety and water is much weaker than for TMAO and its addition to water does not lead to an increase of the solution polarity.[54,94] Hence, our results suggest that the protein stabilization by TMAO is intimately connected to the ability of TMAO to strongly bind water molecules to its hydrophilic group via the indirect mechanisms described above.

VI. CONCLUDING REMARKS

We studied the dynamics of aqueous solutions of trimethylamine-*N*-oxide using a combination of broadband dielectric spectroscopy and polarization-resolved femtosecond vibrational spectroscopy. With both techniques, we find evidence for the existence of stable long-lived TMAO·2H_2O/TMAO·3H_2O complexes. The formation of the complex leads to pronounced parallel dipolar correlations that are reflected in the dielectric spectra of the solutions. The interaction of water with TMAO within the complex is dominated by strong hydrogen-bonds of water to the hydrophilic N−O group of TMAO. The observation of a separate relaxation mode in the dielectric spectra for these complexes shows that TMAO−water hydrogen-bonds have a remarkably long lifetime (>50 ps). Hence, aqueous solutions containing TMAO should be considered as solutions of TMAO·2H_2O/TMAO·3H_2O entities, rather than solutions of isolated TMAO molecules.

Further, the strong hydrogen-bonds of water with TMAO lead to a red-shift of the HDO stretching frequency of these oscillators. These red-shifted HDO molecules give rise to a separate red-shifted band in the infrared spectra. Using time-resolved infrared spectroscopy, we determine the band position to be located at ω = (2450 ± 10) cm^{-1}. We find the vibrational lifetime of these HDO molecules ($\tau_{vib,2}$ = (670 ± 50) fs) to be substantially shorter than observed for bulk-like HDO in water

dx.doi.org/10.1021/jp212542q | J. Phys. Chem. B 2012, 116, 4783−4795

($\tau_{vib,1}$ = (1.8 ± 0.1) ps). The short vibrational lifetime together with a slow component in the heating dynamics of the solutions suggest that excited O−D oscillators bound to TMAO relax efficiently to the vibrational modes of TMAO.

We have also determined the reorientation dynamics of water molecules as measured with dielectric spectroscopy and femtosecond infrared spectroscopy. Both experiments show a slow-down of the rotation of water molecules within the hydrophobic hydration shell of TMAO. In the vicinity of the hydrophilic N−O group of TMAO, 2−3 H_2O molecules are strongly interacting with the solute. This leads to a substantial retardation of their rotational dynamics as reflected in the dielectric spectra. The time-resolved infrared experiments confirm that the O−D groups hydrogen-bonded to TMAO have very slow rotation dynamics, while the O−D oscillators within the complex oriented away from TMAO form the likely origin for the acceleration for a subensemble of O−D groups observed previously and confirmed here.

Finally, we discuss the significance of the strong interaction between water and TMAO for its biological activity. The results imply that strong interaction of the hydrophilic group of TMAO with water is significant for its osmolytic activity. The findings also support the notion of TMAO stabilizing proteins via an indirect mechanism by modifying the polarity and water activity of the solution.

AUTHOR INFORMATION

Corresponding Author

*E-mail: h.bakker@amolf.nl.

Present Address

[‖]Institut de Ciencies Fotoniques, Mediterranean Technology Park, 08860 Castelldefels (Barcelona), Spain.

Notes

The authors declare no competing financial interest.

ACKNOWLEDGMENTS

This work is part of the research program of the *Foundation for Fundamental Research on Matter (FOM)*, which is part of the *Netherlands Organisation for Scientific Research (NWO)*. J.H. thanks the *Deutsche Forschungsgemeinschaft* (DFG) for funding through the award of a research fellowship. We thank Prof. W. Kunz for the provision of laboratory facilities at Regensburg and Dr. Yves Rezus for discussions and providing data.

REFERENCES

(1) Yancey, P. H. *Am. Zool.* **2001**, *41*, 699.
(2) Kempf, B.; Bremer, E. *Arch. Microbiol.* **1998**, *170*, 319.
(3) Daggett, V. *Chem. Rev.* **2006**, *106*, 1898.
(4) Pace, C. N.; Grimsley, G. R.; Scholtz, J. M. In *Protein Folding Handbook*; Buchner, J., Kiefhaber, T., Eds.; Wiley-VCH: Weinheim, Germany, 2005.
(5) Klimov, D. K.; Straub, J. E.; Thirumalai, D. *Proc. Natl. Acad. Sci. U.S.A.* **2004**, *101*, 14760.
(6) Mountain, R. D.; Thirumalai, D. *J. Am. Chem. Soc.* **2003**, *125*, 1950.
(7) Bennion, B. J.; Daggett, V. *Proc. Natl. Acad. Sci. U.S.A.* **2004**, *101*, 6433.
(8) Zou, Q.; Bennion, B. J.; Dagett, V.; Murphy, K. P. *J. Am. Chem. Soc.* **2002**, *124*, 1193.
(9) Fornili, A.; Civera, M.; Sironi, M.; Fornili, S. L. *Phys. Chem. Chem. Phys.* **2003**, *5*, 4905.
(10) Paul, S.; Patey, G. N. *J. Phys. Chem. B* **2006**, *110*, 10514.
(11) Paul, S.; Patey, G. N. *J. Am. Chem. Soc.* **2007**, *129*, 4476.
(12) Laage, D.; Stirnemann, G.; Hynes, J. T. *J. Phys. Chem. B* **2009**, *113*, 2428.
(13) Biyani, N.; Paul, S. *J. Phys. Chem. B* **2009**, *113*, 9644.
(14) Stirnemann, G.; Hynes, J. T.; Laage, D. *J. Phys. Chem. B* **2010**, *114*, 3052.
(15) Kuffel, A.; Zielkiewicz, J. *J. Chem. Phys.* **2010**, *133*, 35102.
(16) Wei, H.; Fan, Y.; Gao, Y. Q. *J. Phys. Chem. B* **2010**, *114*, 557.
(17) Stirnemann, G.; Sterpone, F.; Laage, D. *J. Phys. Chem. B* **2011**, *115*, 3254.
(18) Freda, M.; Onori, H.; Santucci, A. *J. Mol. Struct.* **2001**, *565−566*, 153.
(19) Freda, M.; Onori, H.; Santucci, A. *J. Phys. Chem. B* **2001**, *105*, 12714.
(20) Shikata, T.; Itatani, S. *J. Solution Chem.* **2002**, *31*, 823.
(21) Di Michele, A.; Freda, M.; Onori, G.; Santucci, A. *J. Phys. Chem. A* **2004**, *108*, 6145.
(22) Hovagimyan, K. G.; Gerig, J. T. *J. Phys. Chem. B* **2005**, *109*, 24142.
(23) Sinibaldi, R.; Casieri, C.; Melchionna, S.; Onori, G.; Segre, A. L.; Viel, S.; Mannina, L.; De Luca, F. *J. Phys. Chem. B* **2006**, *110*, 8885.
(24) Rezus, Y. L. A.; Bakker, H. J. *Phys. Rev. Lett.* **2007**, *99*, 148301.
(25) Qvist, J.; Halle, B. *J. Am. Chem. Soc.* **2008**, *130*, 10345.
(26) Panuszko, A.; Bruz'dziak, P.; Zielkiewicz, J.; Wyrzykowski, D.; Stangret, J. *J. Phys. Chem. B* **2009**, *113*, 14797.
(27) Rezus, Y. L. A.; Bakker, H. J. *J. Phys. Chem. B* **2009**, *113*, 4038.
(28) Koga, Y.; Westh, P.; Nishikawa, K.; Subramanian, S. *J. Phys. Chem. B* **2011**, *115*, 2995.
(29) Bakulin, A. A.; Pshenichnikov, S.; Bakker, H. J.; Petersen, C. *J. Phys. Chem. A* **2011**, *115*, 1821.
(30) Pace, C. N.; Marshall, H. F. *Arch. Biochem. Biophys.* **1980**, *190*, 270.
(31) Baskakov, I.; Bolen, D. W. *J. Biol. Chem.* **1998**, *273*, 4831.
(32) Böttcher, C. F. J. *Theory of Electric Polarization*; Elsevier: Amsterdam, The Netherlands, 1978; Vols. *1 and 2*.
(33) Kremer, F., Schönhals, A., Eds. *Broadband Dielectric Spectroscopy*; Springer: Berlin, 2003.
(34) Buchner, R. *Pure Appl. Chem.* **2008**, *80*, 1239.
(35) Buchner, R.; Hefter, G. *Phys. Chem. Chem. Phys.* **2009**, *11*, 8984.
(36) Steinel, T.; Asbury, J. B.; Zheng, J.; Fayer, M. D. *J. Phys. Chem. A* **2004**, *108*, 10957.
(37) Fecko, C. J.; Loparo, J.; Roberts, S. T.; Tokmakoff, A. *J. Chem. Phys.* **2005**, *122*, 54506.
(38) Nibbering, E. T. J.; Fidder, H.; Pines, E. *Annu. Rev. Phys. Chem.* **2005**, *337*, 56.
(39) Bakker, H. J. *Chem. Rev.* **2008**, *108*, 1456.
(40) Bakker, H. J.; Skinner, J. L. *Chem. Rev.* **2010**, *110*, 1498.
(41) Debye, P. *Polar Molecules*; Dover: New York, 1930.
(42) Cavell, E. A. S.; Knight, P. C.; Sheikh, M. A. *Trans. Faraday Soc.* **1971**, *67*, 2225.
(43) Tielrooij, K. J.; Timmer, R. L. A.; Bakker, H. J.; Bonn, M. *Phys. Rev. Lett.* **2009**, *102*, 198303.
(44) Tielrooij, K. J.; van der Post, S.; Hunger, J.; Bonn, M.; Bakker, H. J. *J. Phys. Chem. B* **2011**, *115*, 12638.
(45) Barthel, J.; Bachhuber, K.; Buchner, R.; Hetzenauer, H.; Kleebauer, M. *Ber. Bunsen-Ges. Phys. Chem* **1991**, *95*, 853−859.
(46) Hunger, J. Ph.D. thesis, Regensburg, 2009.
(47) Buchner, R.; Hefter, G.; May, P. M. *J. Phys. Chem. A* **1999**, *103*, 1.
(48) Schrödle, S.; Hefter, G.; Kunz, W.; Buchner, R. *Langmuir* **2006**, *22*, 924.
(49) Buchner, R.; Barthel, J. *Ber. Bunsen-Ges. Phys. Chem.* **1997**, *101*, 1509.
(50) Rezus, Y. L. A.; Bakker, H. J. *J. Chem. Phys.* **2006**, *125*, 144512.
(51) Lin, Y. S.; Pieniazek, P. A.; Yang, M.; Skinner, J. L. *J. Chem. Phys.* **2010**, *132*, 174505.
(52) Tielrooij, K. J.; Petersen, C.; Rezus, Y. L. A.; Bakker, H. J. *Chem. Phys. Lett.* **2009**, *471*, 71.
(53) Timmer, R. L. A.; Tielrooij, K.-J.; Bakker, H. J. *J. Chem. Phys.* **2010**, *132*, 194504.

(54) Tielrooij, K. J.; Hunger, J.; Buchner, R.; Bonn, M.; Bakker, H. J. *J. Am. Chem. Soc.* **2010**, *132*, 15671.
(55) Hunger, J.; Stoppa, A.; Thoman, A.; Walther, M.; Buchner, R. *Chem. Phys. Lett.* **2009**, *471*, 85−91.
(56) Laage, D.; Hynes, J. T. *Science* **2006**, *311*, 832.
(57) Bakker, H. J.; Rezus, Y. L. A.; Timmer, R. L. A. *J. Phys. Chem. A* **2008**, *112*, 11523.
(58) Fukasawa, T.; Sato, T.; Watanabe, J.; Hama, Y.; Kunz, W.; Buchner, R. *Phys. Rev. Lett.* **2005**, *95*, 197802.
(59) Turton, D. A.; Hunger, J.; Hefter, G.; Buchner, R.; Wynne, K. *J. Chem. Phys.* **2008**, *128*, 161102.
(60) Fecko, C. J.; Eaves, J. D.; Tokmakoff, A. *J. Chem. Phys.* **2002**, *117*, 1139.
(61) Zasetsky, A. Y. *Phys. Rev. Lett.* **2011**, *107*, 117601.
(62) Kirkwood, J. G. *J. Chem. Phys.* **1939**, *7*, 911−919.
(63) Fröhlich, H. *Theory of Dielectrics*, 2nd ed.; Oxford University Press: Oxford, U.K., 1965.
(64) Hunger, J.; Stoppa, A.; Buchner, R.; Hefter, G. *J. Phys. Chem. B* **2009**, *113*, 9527.
(65) Quantum mechanical geometry optimizations for TMAO and TMAO·3H_2O were performed using density functional theory (B3LYP[95,96] and PBE[97,98]) and second-order perturbation theory (MP2)[99] as provided by the ORCA program package.[100] For all calculations, the TZVPP basis set[101,102] was used within the resolution of identity.[103,104] Solvation effects were taken into account by the COSMO model[105] taking the dielectric constant of water ε_s = 80 as the permittivity of the medium.
(66) Bevington, P. R. *Data Reduction and Error Analysis for the Physical Sciencies*; McGraw-Hill: New York, 1969.
(67) Note that the reduced error function, χ^2, is normalized to the number of adjustable parameters.[64] Hence, fits using a different number of adjustable parameters are directly comparable.
(68) Buchner, R.; Hölzl, C.; Stauber, J.; Barthel, J. *Phys. Chem. Chem. Phys.* **2002**, *4*, 2169.
(69) Wachter, W.; Buchner, R.; Hefter, G. T. *J. Phys. Chem. B* **2006**, *110*, 5147.
(70) Powles, J. G. *J. Chem. Phys.* **1953**, *21*, 633.
(71) Glarum, S. H. *J. Chem. Phys.* **1960**, *33*, 639.
(72) Linton, E. P. *J. Am. Chem. Soc.* **1940**, *62*, 1945.
(73) Kocherbitov, V.; Veryazov, V.; Söderman, O. *J. Mol. Struct.: THEOCHEM* **2007**, *808*, 111.
(74) The charge transfer of ∼0.1 electron reported by Söderman et al.[73] is also borne out by our calculations.[65]
(75) *Ab initio* calculations for a TMAO·2H_2O complex embedded in a continuum of ε_s = 80 give a smaller dipole moment of $\mu_{eff,\,TMAO\cdot 2H_2O}^{calc}$ = 9.2 D.
(76) Millo, Y.; Raichlin, Y.; Katzir, A. *Appl. Spectrosc.* **2005**, *59*, 460.
(77) Sharp, K. A.; Madan, B.; Manas, E.; Vanderkooi, J. M. *J. Chem. Phys.* **2001**, *114*, 1791.
(78) Rezus, Y. L.; Bakker, H. J. *J. Chem. Phys.* **2005**, *123*, 114502.
(79) Timmer, R.; Bakker, H. J. *J. Chem. Phys.* **2007**, *126*, 154507.
(80) Corcelli, S. A.; Skinner, J. L. *J. Phys. Chem. A* **2005**, *109*, 6154.
(81) Mielke, Z. *Spectrochim. Acta, Part A* **1986**, *42A*, 673.
(82) Munroe, K. L.; Magers, D. H.; Hammer, N. I. *J. Phys. Chem. B* **2011**, *115*, 7699.
(83) Lee, H. S.; Tuckerman, M. E. *J. Chem. Phys.* **2007**, *126*, 164501.
(84) Kast, K. M.; Brickmann, J.; Kast, S. M.; Berry, R. S. *J. Phys. Chem. A* **2003**, *107*, 5342.
(85) Tielrooij, K. J.; Garcia-Araez, N.; Bonn, M.; Bakker, H. J. *Science* **2010**, *328*, 1006.
(86) Ganong, W. F. *Review of Medical Physiology*; McGraw-Hill: New York, 2005.
(87) Meersman, F.; Bowron, D.; Soper, A. K.; Koch, M. H. J. *Biophys. J.* **2009**, *97*, 2559.
(88) Meersman, F.; Bowron, D.; Soper, A. K.; Koch, M. H. J. *Phys. Chem. Chem. Phys.* **2011**, *13*, 13765.
(89) Pace, C. N.; Shirley, B. A.; McNutt, M.; Gajiwala, K. *FASEB J.* **1996**, *10*, 75.
(90) Rose, G. D.; Wolfenden, R. *Annu. Rev. Biophys. Biomol. Struct.* **1993**, *22*, 381.
(91) Levy, Y.; Onuchic, J. N. *Annu. Rev. Biophys. Biomol. Struct.* **2005**, *35*, 389−415.
(92) Cho, S. S.; Reddy, G.; Straub, J. E.; Thirumalai, D. *J. Phys. Chem. B* **2011**, *115*, 13401.
(93) Cordone, L.; Izzo, V.; Sgroi, G.; Fornili, S. L. *Biopolymers* **1979**, *18*, 1965.
(94) Fioretto, D.; Marini, A.; Massarotti, G.; Onori, G.; Palmieri, L.; Santucci, A.; Socino, G. *J. Chem. Phys.* **1993**, *99*, 8115.
(95) Becke, A. D. *J. Chem. Phys.* **1993**, *98*, 5648.
(96) Stephens, P. J.; Devlin, F. J.; Chabalowski, C. F.; Frisch, M. J. *J. Phys. Chem.* **1994**, *98*, 11623.
(97) Pedrew, J. P.; Wang, Y. *Phys. Rev. B: Condens. Matter Mater. Phys.* **1992**, *45*, 13244.
(98) Perdew, J. P.; Burke, K.; Ernzerhof, M. *Phys. Rev. Lett.* **1996**, *77*, 3865.
(99) Head-Gordon, M.; Pople, J. A.; Frisch, M. J. *Chem. Phys. Lett.* **1988**, *153*, 503.
(100) Neese, F. *Wiley Interdiscip. Rev.: Comput. Mol. Sci.* **2012**, *2*, 73.
(101) Schäfer, A.; Horn, H.; Ahlrichs, R. *J. Chem. Phys.* **1992**, *97*, 2571.
(102) Weigend, F.; Ahlrichs, R. *Phys. Chem. Chem. Phys.* **2005**, *7*, 3297.
(103) Nesse, F. *J. Comput. Chem.* **2003**, *97*, 2571.
(104) Vahtras, O.; Almlöf, J.; Feyereisen, M. W. *Chem. Phys. Lett.* **1993**, *213*, 514.
(105) Sinnecker, S.; Rajendran, A.; Klamt, A.; Diedenhofen, M.; Nesse, F. *J. Phys. Chem. A* **2006**, *110*, 2235.